DIAGNOSTIC NUCLEAR MEDICINE

Quantitative Analysis of Left-Ventricular Function Using Gated Single Photon Emission Tomography

Jean-Louis Barat, A. Jacques Brendel, Jean-Pierre Colle, Vincent Magimel-Pelonnier, Joël Ohayon, Sinclair Wynchank, Françoise Leccia, Pierre Besse, and Dominique Ducassou

Hôpital Universitaire du Haut Lévêque, Bordeaux France

We describe a quantitative method that measures segmental motion of the left ventricle, using tomographic slices obtained by gated single photon emission tomography (GSPECT). These slices contain the major axis of the left ventricle and are presumed to show wall motion directed towards a center of contraction. Values of parameters describing segmental wall motion in GSPECT were obtained from 61 patients, who received a left cardiac catheterization 1 hr later. These values were compared with results of similar calculations applied to data from contrast ventriculography. We conclude that GSPECT allows a detailed and quantitative, noninvasive study of wall motion of all left ventricular segments, with high inter- and intraobserver reproducibility.

J Nucl Med 25: 1167–1174, 1984

Quantitative analysis of left-ventricular global and segmental function has become an important tool for the objective assessment of ventricular performance after ischemic heart disease and therapeutic intervention. In this field planar radionuclide ventriculography has been shown to be sensitive, with the advantage of being very much less invasive than contrast ventriculography (*1–3*). To evaluate quantitative parameters such as global or regional ejection fraction, the background activity must be determined. Usually a correction is made for overlapping background by subtraction of a single threshold whose magnitude is estimated from a sampling region that avoids large vascular structures. The true background correction, however, requires three-dimensional reconstruction. In addition, equilibrium gated planar ventriculography cannot avoid the superposition of counts from different depths within the same cavity. Therefore a quantification of regional motion from planar scintigraphy can give only an overall result. Emission tomography of the cardiac cavities overcomes these problems of background and superposition, and offers a promising, precise technique for noninvasive assessment of wall motion and chamber volumes.

Several preliminary studies have already shown the ability of gated single photon emission computed tomography (GSPECT), to demonstrate qualitatively disorders of wall motion or to measure relative parameters like global ejection fraction (*4–7*). In the work described here we have attempted to establish a method for objective quantitative analysis of wall motion using GSPECT, and also to assess it in terms of contrast angiocardiography.

Received July 25, 1983; revision accepted July 13, 1984.

For reprints contact: J. L. Barat, PhD, MD, Service de Médecine Nucléaire, Hôpital Universitaire du Haut Lévêque, 33600 Bordeaux Pessac, France.

MATERIAL AND METHODS

Gated single photon emission tomography. The single photon emission tomograph used in this investigation consisted of a large-field-of-view gamma camera, 40 cm in diameter. It is mounted on a gantry that rotates through 360° about the patient, and it is interfaced to a computer equipped with an array processor.*

A low-energy parallel-hole collimator was used, giving an overall spatial resolution of 10 mm FWHM (in air) at a distance of 10 cm from the collimator. The effective resolution under conditions comparable to those of the clinical studies was measured using Tc-99m-filled cap-

illary tubes in a phantom representing a human thorax, whose cross section is an ellipse having major axis 32 cm and minor axis 22 cm. It was filled with stearin beads whose coefficient of absorption for 140-keV photons is approximately equal to that of lungs with appropriate proportions of thoracic muscle. With the camera moving in an orbit with radius 23 cm, we found, after reconstruction, a resolution of 19 mm FWHM near the axis of revolution in a transverse plane, and 20 mm FWHM along the axis of revolution. The patient's red blood cells were labeled with 25 mCi [Tc-99m]pertechnetate, using an in vivo method.

ECG-gated data were acquired during all of the 360° orbit during 20 min. They were stored in 64-by-64 matrices, obtained from 64 angular projections. The framing rate was 8 frames per cardiac cycle. The mean cycle length was determined from the average duration of 32 cardiac cycles recorded just before the start of data acquisition. The histogram of these cycles was displayed on the image screen and patients presenting arrhythmias corresponding to more than 15% of the mean cycle duration were excluded from the study. Correction for loss of data in the last frame due to short cardiac cycles within this beat range, and for different numbers of cycles acquired in each projection, was made by recording the number of cycles sampled in each interval and normalizing on this basis after the end of data acquisition. In all, 512 images were obtained comprising 8 cine frames for each of the 64 angular projections. The maximum number of cardiac cycles (M) contributing to one of these images was selected. The normalizing factor for image data was the ratio of M to the number of cycles contributing to a particular image.

The count rate usually ranged from 16,000 to 22,000 cps, so a total of $\simeq$ 3 million events were collected for each eighth of the resultant cardiac cycle. From an anterior view, the level of a set of transverse sections one pixel thick (i.e., 6 mm) was selected.

The data were then filtered and back-projected, using the manufacturer's software. No attenuation correction was made. For 16 slices and 8 frames per cardiac cycle, the total processing time was 6 min. Sagittal slices parallel to the long cardiac axis, and coronal slices parallel to the short axis, were then obtained, requiring 20 sec per slice. A Fourier analysis of the time variation over the cardiac cycle was then performed for each pixel of a given slice. This allowed images to be constructed for each slice, representing the phase and amplitude of the first harmonic of the Fourier series. In this work we have restricted our analysis to sagittal slices containing the long axis of the left-ventricular (LV) cavity.

Contrast angiocardiography. Contrast ventriculograms in 30° RAO projection were obtained after injecting contrast material at 15 ml/sec through a "pigtail" catheter into the LV cavity. The recording rate of the camera was 50 frames/sec. Imaging of a 1-cm square grid at the level of the heart allowed further correction for magnification and distortion. Finally, coronary angiography was performed.

Patient selection. Sixty-six patients, referred because of chest pain, were examined by contrast left ventriculography (CLV) and coronary arteriography. They had undergone GSPECT one hour earlier. Five cases were excluded because insufficient opacification of the LV. Both examinations were performed in the morning, with all medication discontinued the previous evening.

Data processing. Segmental analysis of the LV wall motion was performed for both CLV and GSPECT, following a method first introduced by the Stanford group (*8*) to describe LV motion from contrast ventriculograms in the 30° RAO projection. Assuming that systolic wall motion was directed towards a center of contraction inside the LV, they found this center to be situated on the segment joining the superior aspect of the aortic valve to the apex in end-systole. Its locus divided the segment in the ratio 69:31 from the aortic valve. This site for the center of contraction yielded the minimum error from 1400 tested points, in a study performed with midwall implanted markers (*8*).

In CLV studies using the 30° RAO projection, cine film was replayed in a frame-by-frame manner, and end-diastolic (ED) and end-systolic (ES) images of the same contraction, far remote from any premature ventricular contraction, were selected. ED and ES frames were identified on the basis of maximum and minimum area of the LV cavity. The ES image was selected from the frame just before the onset of outward motion of the ventricular walls. The coordinates of the ED and ES outlines were digitized using an ultrasonic pen, and then transmitted to a computer. Also transmitted were coordinates of the apical dimple, the LV-aortic junction, the center of the image intensifier, and reference points on the image of the grid, 5 cm from the center. In the first step of data processing, corrections were made for distortion and magnification. Then the center of contraction was located, as described above. From this center, ten uniformly spaced sectors were automatically drawn and superimposed on the outlines of ED and ES. The sectors were oriented with respect to cardiac anatomic features, as shown in Fig. 1. The segmental wall motion was measured as the percentage of shortening of each sector's mean radius (SRS).

For comparison with CLV studies in the 30° RAO projection, a GSPECT long-axis sagittal slice along the LV major axis was reconstructed. The slice thickness was usually 2 pixels (12 mm). For large hypokinetic cavities, 3-pixel slices gave better statistical accuracy without affecting the precision of the segmental analysis. Areas of interest corresponding to the LV were obtained as the regions enclosed between the LV free borders in the ED and ES frames, chosen along an appropriate isocount contour, and a curve representing the basal limits of the

LV. Phantom studies were performed using balloons, 50 to 300 ml in volume, filled with radioactive water, and placed in the stearin scattering medium, and these established the isocount value to be nearly constant and equal to 30% of the maximum count value within the cavity. The LV base could not be clearly recognized in images of blood-pool activity, so the Fourier analysis, displaying amplitude and phase, was used to obtain the functional limit between LV and left atrium (minimum amplitude and abrupt phase shift of 180°). This contour defined the LV basal border. On the ES display, a light-pen was used to identify both the anterior LV-aortic junction and the apex; the center of contraction was then located on the segment joining these two points, at 69% of the distance from the LV-aortic end. An identical sectorial segmentation was performed as before, and the wall motion was expressed in terms of the fractional change in counts between diastole and systole in each sector. This is the sectorial ejection fraction, SEF.

Interobserver comparison. The interobserver reproducibility for each technique was evaluated in the following way. Two pairs of experienced observers, who were independent and "blinded," obtained results for SEF from GSPECT studies (Observers 1 and 2, n = 27) and for SRS from CLV (Observers 3 and 4, n = 15), from a sequential set of otherwise unselected patients. Using a linear regression technique, values for each sector from each study obtained by the pair of observers were analyzed (i.e., Observer 1 compared with 2 and Observer 3 compared with 4). Then the significance of the difference between the resulting lines and the line of identity was tested.

Intraobserver variation. A similar approach was used to check the intraobserver variation of each technique and for each sector. After a delay of 3 mo, data obtained from the same consecutive series of patients were reworked by two "blinded" observers. Observer 1 reviewed and recalculated GSPECT data, and Observer 3 did the same for CLV. The pairs of values of SEF obtained by Observer 1 from the original and repeated data processing were analyzed for each sector using a linear regression technique. A similar analysis was done for the pairs of value of SRS obtained by Observer 3. The results were treated as for the interobserver comparison.

RESULTS

The 61 contrast left ventriculograms covered a wide spectrum of normal and abnormal contraction patterns. Ten patients had normal LV contraction and no coronary artery disease. Nine demonstrated single-vessel stenosis, but without any impairment of LV function. Four had mitral-valve prolapse and associated hyperkinesis. Four showed diffuse hypokinesis due to nonobstructive cardiomyopathy. Finally, 34 displayed abnormal contraction after an infarct due to coronary artery thrombosis.

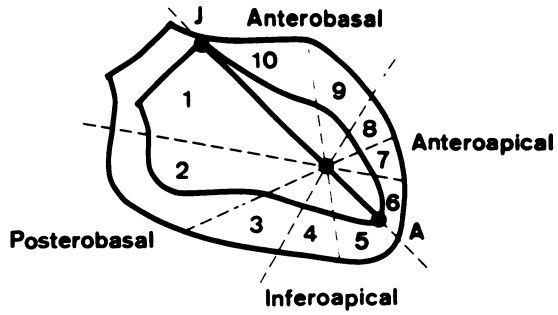

FIG. 1. Cardiac outlines at ED and ES. Center of contraction is on line joining LV-aortic junction (J) to apex (A), as described in text; it forms center of ten 36° radial sectors. These are grouped into four conventional anatomic regions, whose adjacent names include sectors as follows: posterobasal (*2,3*), inferoapical (*4,5*), anteroapical (*6,7,8*) and anterobasal (*9, 10*).

Figure 2 gives examples of images for patients showing normal and abnormal ventricular function, obtained from CLV and GSPECT.

Correlation between motion of segments as demonstrated by GSPECT and CLV. Mean values and ranges of GSPECT sectorial ejection fractions are given in Table 1. Also in this table there are the ranges and mean values of the shortening of the average radii for each segment, obtained from contrast ventriculography in 30° RAO view. The large ranges reflect the great variation of observed wall motion.

The correlation between the pairs of measured quantities was analyzed using a linear regression technique, which is justified below. The slope and intercept of the regression line are given for each sector. Also the standard error of the estimate (s.e.e.) and correlation coefficients (r) are listed.

Of the ten sectors examined within the LV, Sector 1 represents the aortic-valve region. Among contractile zones, the inferobasal (Sector 2) gives the lowest correlation coefficient (0.56) while the anteroapical zone (Sector 6) gives 0.78, the highest. The values of SEF obtained from SPECT are plotted against SRS (CLV) in Fig. 3 for these two sectors.

Inter and intraobserver variations for both GSPECT and CLV. The interobserver comparison for each technique used a linear regression analysis, with results given in Table 2. The two pairs of observers (1 and 2 for GSPECT and 3 and 4 for CLV) produced pairs of results for each sector. The slopes and intercepts of the regression lines are given. In all cases except one (CLV Sector 1) the slopes of the fits do not differ significantly from 1.0, nor the intercepts from 0.0. The interobserver variation is also given in this table as the standard deviation (σ_x for CLV and σ_y for GSPECT) of the population of the differences between each pair of values. An estimate of the overall interobserver variance when comparing GSPECT and CLV ($\sigma^2 = \sigma^2_x + \sigma^2_y$) is given in the last line of the table. Depending on the sector, σ^2 varies between 27% and 59% of (s.e.e.),[2] derived from

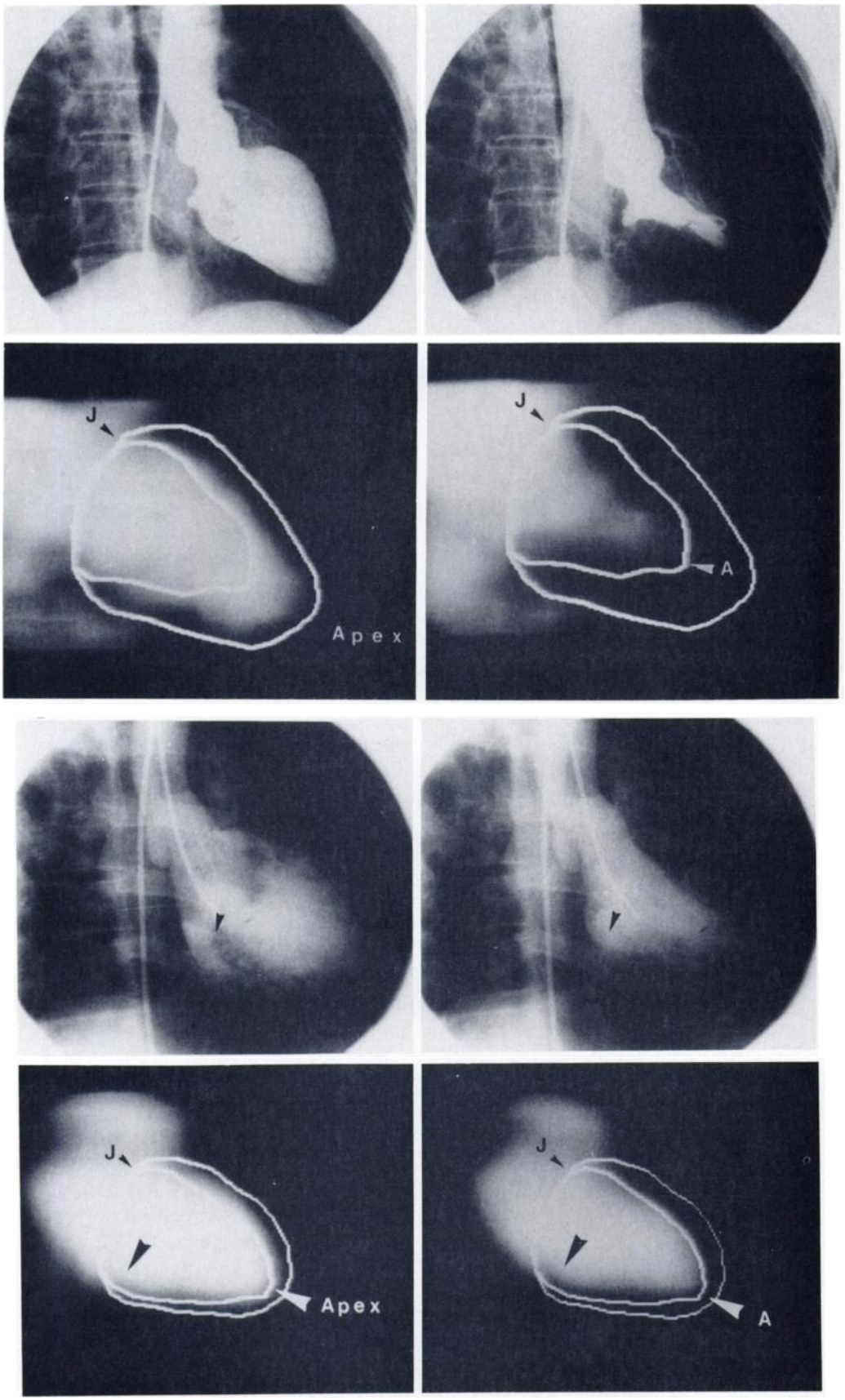

FIG. 2. Images from two patients: upper 4 normal, lower 4 showing inferobasal akinetic region due to infarct (arrow). Left column diastolic, right systolic. Lines 1 and 3 from contrast ventriculography, 30° RAO; lines 2 and 4 from GSPECT, sagittal slice containing long LV axis.

TABLE 1. CORRELATIONS BETWEEN MOTION OF LV SEGMENTS AS DEMONSTRATED BY GSPECT AND CLV FOR 61 PATIENTS.

Sector	1	2	3	4	5	6	7	8	9	10
Mean SEF*	23.6	26.5	35.5	35.8	37.9	35.9	35.3	35.9	40.5	38.4
SEF* range	1–52	0–53	−2–83	−8–89	−8–89	−8–88	−12–86	−7–83	−8–80	1–65
Mean SRS†	10.7	19.7	33.1	32.2	26.6	26.3	35.5	39.8	42.0	37.5
SRS† range	0–34	0–47	−11–71	−22–70	−11–67	−14–74	−22–86	−21–88	−8–88	11–75
Slope b‡	1.00	0.75	0.74	0.81	0.96	0.92	0.70	0.64	0.68	0.61
Intercept a‡	12.8	11.7	11.0	9.8	12.3	11.7	10.3	10.6	11.7	15.3
s.e.e.§	10.8	12.4	16.3	17.7	17.1	16.7	17.4	18.0	17.5	14.7
r¶	0.45	0.56	0.69	0.68	0.74	0.78	0.74	0.69	0.70	0.58

* SEF is Sectorial Ejection Fraction obtained from GSPECT.
† SRS is Sectorial mean Radius Shortening obtained from CLV.
‡ Linear regression analysis uses equation $y = a + bx$, where y = SEF and x = SRS.
§ S.e.e. is standard error of estimate (σ_{xy}).
¶ r is correlation coefficient.

the regression analysis of SEF (GSPECT) compared with SRS (CLV). This estimate gives an indication of how the interobserver variation contributes to the dispersion of the points when the two techniques are correlated.

The results of an identical treatment to evaluate the intraobserver variation for both techniques are given in Table 3. Data from the same consecutive group of patients were reprocessed by the same observer 3 mo after the first analysis. This was repeated for each technique. The pairs of values (from Analyses 1 and 2) were examined by linear regression analysis. The regression lines for each sector and technique do not differ significantly from the line with slope unity and zero intercept. The table includes the standard deviations (σ'_x for CLV, and σ'_y for GSPECT) of the population of differences between pairs of values. This allows an estimate of the overall intraobserver variance $\sigma'^2 = \sigma'^2_x + \sigma'^2_y$ for each sector. The intraobserver variation contributes to the dispersion of the points used for the linear regression analysis of SEF (GSPECT) compared with SRS (CLV). Its effect is seen in the intraobserver overall variance, σ'^2, which ranges from 7% to 37% of $(\text{s.e.e.})^2$ for the different sectors.

DISCUSSION

A study of segmental ventricular function is of particular interest in patients who have lesions of the coronary arteries. It may either aid the evaluation of the extent of malfunction or monitor therapy. Contrast angiography remains the reference method for analysis of ventricular function. Although its usefulness is limited by its invasive nature, this does not apply to radionuclide ventriculography. But whichever technique is used, it has been shown (*9–12*) that inter- and intraobserver variations limit the quality of results obtained from merely visual interpretation of angiograms or scintigraphic data. A quantitative analysis of ventricular function is therefore justified, not only because it is more objective but also more reproducible. Radionuclide investigation of

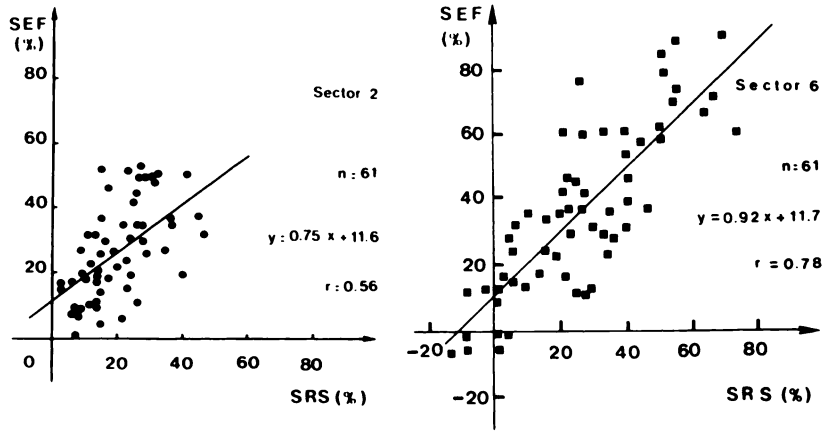

FIG. 3. Plot of sectorial ejection fractions (SEF), from GSPECT, against sectorial radius shortening (SRS) from CLV, for Sectors 2 (inferobasal, left) and 6 (anteroapical, right).

TABLE 2. INTEROBSERVER COMPARISON FOR EACH LV SECTOR FROM BOTH GSPECT AND CLV

Sector	1	2	3	4	5	6	7	8	9	10
GSPECT results (Observers 1 compared with 2)										
N = 27*										
Slope	1.08	0.92	0.96	1.02	0.99	0.98	0.91	1.01	1.02	1.08
Intercept	−0.2	1.9	2.0	0.6	0.6	1.7	3.9	−0.1	−1.5	0.6
r	0.96	0.97	0.98	0.99	0.99	0.97	0.96	0.99	0.99	0.97
σ_y	2.8	2.2	2.8	3.0	1.7	5.2	4.9	2.2	2.8	3.7
CLV results (Observers 3 compared with 4)										
N = 15*										
Slope	0.92	1.17	1.16	1.14	1.16	1.05	0.95	0.87	0.76	0.79
Intercept	3.8 (NS)	−0.9	−9.4	−3.1	−0.8	5.0	0.6	7.0	12.6	7.9
r	0.54	0.74	0.91	0.91	0.85	0.88	0.92	0.77	0.77	0.68
σ_x	4.9	7.9	9.3	8.9	11.5	11.2	8.7	13.1	12.6	10.7
$\sigma^2 = \sigma_x^2 + \sigma_y^2$	32	67	94	88	135	152	96	176	167	128
σ^2 as % (s.e.e.)^2 from Table 1	27	44	35	28	46	55	32	54	54	59

* Sequential set of otherwise unselected patients.

TABLE 3. INTRAOBSERVER COMPARISON FOR EACH LV SECTOR FROM BOTH GSPECT AND CLV

Sector	1	2	3	4	5	6	7	8	9	10
GSPECT results										
Observer 1 (first analysis compared with second)										
n = 24*										
Slope	0.91	1.02	1.00	1.00	1.04	1.03	1.01	1.04	0.98	0.92
Intercept	0.6	−1.1	0.2	0.2	−1.4	−0.3	1.1	1.1	2.1	4.4
r	0.94	0.93	0.98	0.99	0.99	0.99	0.98	0.98	0.96	0.95
σ'_y	2.3	3.4	2.8	2.6	2.5	2.8	3.3	3.2	4.5	3.6
CLV results										
Observer 3 (first analysis compared with second)										
n = 12*										
Slope	0.92	0.40	0.89	0.89	0.93	0.99	0.95	0.95	0.95	0.90
Intercept	1.1	11.0	3.2	4.3	3.4	0.1	1.4	0.2	−0.6	4.2
r	0.96	0.75	0.96	0.95	0.93	0.92	0.95	0.97	0.97	0.90
σ'_x	1.6	2.6	4.2	4.6	5.7	9.7	8.3	6.2	5.6	7.0
$\sigma'^2 = \sigma'^2_x + \sigma'^2_y$	8	18	25	28	39	102	80	49	52	62
σ'^2 as % (SEE)^2 from Table 1	7	12	9	9	13	37	26	15	17	29

* Sequential set of otherwise unselected patients.

ventricular motion can be performed with a conventional gamma camera using different views, after a single radioactive injection. This is a gated equilibrium study, and it can be analyzed qualitatively in terms of the ventricular function in different regions. This has proved very useful in certain cases, especially when there is a significant anomaly of wall motion. But because of the presence of radiotracer throughout the vascular system, a superposition of other heart chambers on the left ventricle occurs in all views except LAO. Even using this

view there remains a superposition of the different planes within the LV. Hence a quantification of regional motion from planar scintigraphy can give only an overall result.

This problem of superposition is overcome by use of a conventional gamma camera that rotates around the patient and uses GSPECT tomography. Thus quantification of the motion for any ventricular segment is possible in any reconstructed slice. The method of describing wall motion towards a center of contraction, as defined by the Stanford group, has been shown to have better diagnostic capabilities than other methods so far proposed (*13*). A radial method for analysis is well suited to the radioactive technique, whether planar or tomographic, because it allows a description of the motion in terms of a sectorial ejection fraction, the apices of the sectors being at the presumed center of contraction. The present work used this principle, both in GSPECT, which examines a vertical slice containing the long axis of the cavity, and in CLV using a 30° RAO projection. A correlation has been sought between the measured segmental movements, to determine the ability of GSPECT to represent actual motion. We have found the correlation coefficients for different sectors to vary from 0.56 to 0.78. In fact, the analytical method used for the two techniques was semiautomatic. The observer was required to intervene at different stages during data processing. This could provide intra- and interobserver variation. For CLV the operator must define the cavity contour. Precautions were taken to reduce errors, as by the exclusion of five cases in which the ventricle was insufficiently opacified. Also a contour was chosen along the line of maximum contrast, thus smoothing the irregularities at the cavity's edge. By this procedure the papillary muscles were excluded. With GSPECT ventriculography the contours of the cavity in diastole and systole were automatically traced using an isocontour that followed the anterior, apical, and inferior edges of the cavity and using a functional boundary along the base. For both techniques, shape recognition is necessary. This is difficult to automate. Two anatomic landmarks must be recognized: the anterior ventriculoaortic junction and the apex. The inter- and intraobserver variations shown in Tables 2 and 3 are explained by the list of operator decisions enumerated above. The analysis of CLV data relies more on such operator intervention, hence the estimated variances for CLV are greater. We have shown, however, that the order of magnitude of global interobserver variance does not exceed 59% of the variance estimated from the linear regression analysis comparing the two techniques. Thus other possible causes of variation must be considered:

1. In this work the effect of clinical changes was diminished by minimizing the time interval between the two studies. But variations in the conditions under which data are recorded cannot always be totally eliminated.

2. Quantitative analysis from contrast ventriculography depends on measurements obtained during a single cardiac cycle, in particular one well away from a premature ventricular contraction. The chosen cycle can differ from the averaged cycle (resulting from about 1200 cycles) that is used to provide a tomographic slice with GSPECT. The solution to this problem would be to analyze several cycles observed with CLV and to establish means of sectorial shortening. In practice this was not possible with the 61 patients. Many of the angiograms showed induced arrhythmias or unsatisfactory opacification in cycles after the first.

3. The chosen end-systolic image on the contrast angiogram was the frame giving the minimal LV area and preceding the onset of outward motions of the ventricular walls. But there are frequently slight temporal differences in the motion of various walls. Thus the global minimal volume may not necessarily correlate with the maximal inward motion of a particular wall. This could account for additional variability when comparing GSPECT and CLV.

4. The framing rate used in the GSPECT study described here was only 8 frames per cardiac cycle, which corresponds to a time resolution of about 100 ms per frame. This was done to achieve enough counts in spite of the constraints imposed by the maximum injected dose and examination length. It is clear that this framing rate is insufficient if an analysis of time-activity curves is required, for example to determine parameters of ventricular filling such as peak ejection or filling rates. But our analysis is aimed only at regional ejection fractions. We have measured the effect of this time resolution on global ejection fraction, obtained by gated equilibrium planar ventriculography. In a series of 17 consecutive patients at rest, data were first acquired with a framing rate of 16 per cardiac cycle and then with 8 frames per cycle. The faster rate, which corresponds to a time resolution of about 50 ms, is generally accepted as sufficient for a measurement of ejection fraction. As expected, the ejection fractions measured from the slower framing rate were significantly ($p < 0.01$) and consistently lower, with a mean difference of 4.8% relative EF units. This result agrees with those of the Duke or Seattle groups (*14,15*). The effect of this framing rate is a systematic underestimation of the ejection fraction and should have little consequence on correlation between GSPECT and CLV.

5. Another problem arises from the fact that on the GSPECT slice chosen, the basal limits of the LV are chosen as functional limits, by means of Fourier analysis images showing minimum amplitude and a phase change of 180°. This contour is taken as fixed during the cardiac cycle. But in fact the plane of the mitral valve moves towards the apex during systole. This may in part explain disagreement between the two analytical techniques, particularly in Sector 2 (inferobasal), where the correlation coefficient is only 0.56.

6. A further point to be considered is justification for using linear regression analysis to compare SEF obtained from GSPECT, with SRS provided by CLV. If we suppose that the observations are made in a single infinitely thin plane, then SEF is related to the square of SRS. (cf. Appendix). However, a long-axis sagittal slice obtained from GSPECT has a thickness of 12 to 18 mm. Similarly the edge of a cavity, displayed by CLV, results from the superposition of a large number of plane projections, hence the above theoretical relationship cannot be considered. The empirical relation between ejection fraction and radius shortening in general was found in the following way. Using the contrast angiographic data, the global ejection fraction was obtained using Simpson's rule, and the averaged sectorial shortening was also calculated. A linear relation was demonstrated between these two quantities, which depends on data obtained from the same measurement (n = 45, slope = 0.93, intercept = 29.0, s.e.e. = 7.2, and r = 0.92). Hence it is likely that SEF and SRS, which were obtained by the two techniques under consideration, are similarly related.

Analysis described here has been limited to dynamic studies in a vertical plane that includes the major axis of the cavity. In fact this method can be applied to any plane containing this axis—in particular, a reoriented transverse plane giving an apical 4-chamber view. This will allow examination and quantification of movement in the septal and posterolateral segments.

In conclusion, quantitative evaluation of segmental cardiac kinetics allows an objective assessment of cardiac function. Our method, based on a center of contraction, has the advantage of being simple. It allows GSPECT to describe and quantify localized movements of the inner myocardial surface with reference to results from contrast angiography. The value of GSPECT has been clearly demonstrated, and its results correlate with contrast ventriculography. For this reason—and especially because of its noninvasive nature—it is likely that GSPECT will prove very useful in investigations of myocardial function.

FOOTNOTE

* CGR Gammatome, 75736 Paris Cedex 15, France.

ACKNOWLEDGMENTS

The authors thank most warmly M. D. Commenges for fruitful discussions concerning the statistical analysis within this work, Miss M. P. Isidore, and MM. F. Lacroix and A. Descamps for their technical aid, and Mrs. M. Rouais for her secretarial assistance.

APPENDIX

In a single, infinitely thin plane:

$$SEF = (Sd - Ss)/Sd,$$

where S is the area of the sector in diastole (d) or systole (s) and is given by:

$$S = \tfrac{1}{2}\,\alpha r^2_m,$$

with α the angle of the sector and r_m the mean radius, with values r_{md} and r_{ms} in diastole and systole. Similarly

$$SRS = (r_{md} - r_{ms})/r_{md}.$$

Hence the relation between SEF and SRS is:

$$SEF = SRS\,(2 - SRS).$$

REFERENCES

1. MARSHALL RC, BERGER HJ, COSTIN JC, et al: Assessment of cardiac performance with quantitative radionuclide angiocardiography. *Circulation* 56:820-829, 1977
2. BODENHEIMER MM, BANKA VS, FOOSHEE CM, et al: Comparison of wall motion and regional ejection fraction at rest and during isometric exercise: Concise communication. *J. Nucl Med* 20:724-732, 1979
3. BRADY TJ, THRALL JH, KEYES JW, et al: Segmental wall-motion analysis in the right anterior oblique projection: comparison of exercise equilibrium radionuclide ventriculography and exercise contrast ventriculography. *J Nucl Med* 21:617-621, 1980
4. MOORE ML, MURPHY PH, BURDINE JA: ECG-gated emission computed tomography of the cardiac blood pool. *Radiology* 134:233-235, 1980
5. PHILIPPE L, ITTI R, LORGERON JM, et al: Thick slice emission tomography for quantitative assessment of cardiac function. *J Nucl Med* 23:P61, 1982 (abst)
6. MAUBLANT J, BAILLY P, MESTAS D, et al: Feasibility of gated single-photon emission transaxial tomography of the cardiac blood pool. *Radiology* 146:837-839, 1983
7. TAMAKI N, MUKAI T, ISHII Y, et al: Multiaxial tomography of heart chambers by gated blood-pool emission computed tomography using a rotating gamma camera. *Radiology*, 147:547-554, 1983
8. INGELS NB, DAUGHTERS GT, STINSON EB, et al: Evaluation of methods for quantitating left ventricular segmental wall motion in man using myocardial markers as a standard. *Circulation* 61:966-972, 1980
9. LEIGHTON RF, WILT SM, LEWIS RP: Detection of hypokinesis by a quantitative analysis of left ventricular cineangiograms. *Circulation* 50:121-127, 1974
10. CHAITMAN BR, DEMOTS H, BRISTOW JD, et al: Objective and subjective analysis of left ventricular angiograms. *Circulation* 52:420-425, 1975
11. ZIR LM, MILLER SW, DINSMORE RE, et al: Interobserver variability in coronary angiography. *Circulation* 53:627-632, 1976
12. OKADA RD, KIRSHENBAUM HD, KUSHNER FG, et al: Observer variance in the qualitative evaluation of left ventricular wall motion and the quantitation of left ventricular ejection fraction using rest and exercise multigated blood pool imaging. *Circulation* 61:128-136, 1980
13. COLLE JP, LE GOFF G, PAGE A, et al: Validité de la méthode de Stanford dans l'évaluation des dyskinesies segmentaires du ventricule gauche. *Arch Mal Coeur* 4:395-405, 1982
14. BOWYER KW, KONSTANTINOW G, RERYCH SK, JONES RH: Optimum counting in radionuclide cardiac studies. In *Nuclear Cardiology Selected Computed Aspects.* New York, Society of Nuclear Medicine, 1978, pp 85-95
15. HAMILTON GW, WILLIAMS DL, CALDWELL JH: Frame rate requirements for recording time activity curves by radionuclide angiocardiography. In *Nuclear Cardiology Selected Computed Aspects.* New York, Society of Nuclear Medicine, 1978, pp. 75-83.